HiSST: 3rd International Conference on
High-Speed Vehicle Science Technology
14 -19 April 2024, Busan, Korea

Numerical Study of Vitiation Air Effects on the Hydrogen-fueled Direct-Connect Scramjet Combustor

Seung-Min Jeong[1], Jae-Eun Kim[2], Min-Soo Kim[3], Jeong-Yeol Choi [4]

Abstract

This study numerically investigates the combustion characteristics of a hydrogen-fueled scramjet combustor by incoming vitiation air effects. A high-resolution comprehensive numerical simulation was conducted with hybrid LES/RANS and high-order schemes. Two different global equivalence ratios, 0.23 and 0.45, were applied on each incoming air condition, clean air and vitiation air, to investigate the effects of equivalence ratio changing. The results show that shock trains accompanied by a thermal chocked formed around the cavity close-out region when the incoming flow condition changes from vitiated air to clean air condition. The change in combustion characteristics depending on the incoming air was found to be more severe as the equivalence ratio increased. Present results indicate that when the ground experimental test with the vitiated air heater to derive the design point of a scramjet combustor or engine, results must be calibrated considering the discrepancies between the combustion characteristics of the clean and vitiated air.

Keywords: *Direct-Connect Scramjet Combustor, Vitiated Air Heater, Vitiation Air Effect, High-resolution Numerical Simulation*

1. Introduction

A facility that can provide high-enthalpy, high-Mach number flow to test the hypersonic propulsion system, such as ramjet, scramjet, and dual-mode scramjet engines on the ground experimentally, is required. In the ground test, several types of facilities have been used to simulate supersonic conditions with a high enthalpy flow condition. These can be categorized as storage air heater (SAH), electrical resistance heater (EAH), and vitiation air heater (VAH). In particular, VAH has been widely adopted due to its relatively easy installation and operational convenience.

However, because the VAH uses combustion to make up high enthalpy flow, it is unavoidable for the combustion product, such as H2O or CO, to be included in the high enthalpy flow. Therefore, several experimental and numerical studies have been conducted to describe the vitiated air effect on a flame structure, combustion dynamics, and engine performance [1-6]. As several study reported, the combustor flow field exhibits significant variations depending on the incoming air condition. Efforts have been made recently to schematize and predict these relationships; however, this requires detailed combustion properties within the combustor based on various and numerous data. Therefore, comprehensive numerical simulations with high-fidelity are needed to understand these detailed field data, but due to realistic problems.

The present study conducted a high-resolution comprehensive numerical simulation on a hydrogen-fueled direct-connect scramjet combustor to investigate the vitiated incoming air effects from the fluid

[1] *Postdoctoral Researcher, Aeropropulsion Research Division, Korea Aerospace Research Institute, smjeong@kari.re.kr*
[2] *Graduate Researcher, M.S., Department of Aerospace Engineering, Pusan National University*
[3] *Doctoral Student, Department of Aerospace Engineering, Pusan National University*
[4] *Professor, Department of Aerospace Engineering, Pusan National University, aerochoi@pusan.ac.kr*

and combustion dynamics perspective. It is the preliminary stage of the construction of a calibration tool that aims to derivate a combustion flow field or performance based on clean air condition from data accumulated using vitiated air condition.

2. Methodology

2.1. Governing Equation and Numerical Approach

A density-based, fully compressible reactive in-house code ("PNURPL3DFR") was used in the present research. A chemical species, momentum, energy, and turbulent transport equation, in which a fluid and chemical reaction are fully coupled, were used as the governing equations. All equations were treated using the finite volume method and based on a fully structure grid. A density was calculated by the sum of the partial density of each species. The temperature was calculated using the total energy and temperature relationship with a Newton-Raphson iterative approach. The pressure was calculated using an ideal gas equation of state (EoS). Several previous numerical studies have noted more detailed numerical framework information of "PNURPL3DFR" [7-16].

Jachimowski detailed the hydrogen/air chemical reaction mechanism [17], which consists of 8 species and 19 reaction steps, was selected. Including nitrogen as an inert gas, so the total number of species is nine. Owing to sufficient fine grid level with a small volume (O(100 cm^3)), the present study selected the "quasi-laminar approach", instead of applying a turbulent-combustion model, such as a partially stirred reactor (PaSR) [18,19].

The present study used an improved delayed detached eddy simulation (IDDES) model, which controlled grid-induced separation (GIS) problem in delayed detached simulation (DES), and solved log-layer mismatch (LLM), which is a hazard problem in delayed detached eddy simulation (DDES). In order to derive high-resolution results, spatial reconstruction was treated by the fifth-order accurate, optimized multi-dimensional limiting process (oMLP) method. Previous study confirmed that the oMLP scheme performs better than the weighted essentially non-oscillatory (WENO) scheme [20]. Viscous flux was calculated using the fourth-order central difference method, and the AUSMPW+ scheme treated flux splitting. Second-order accurate, fully implicit optimized lower-upper symmetric gauss-seidel (LU-SGS) scheme with a maximum four-step Newton sub-iteration method was used as a time marching scheme.

2.2. Combustor Model and Working Fluid Conditions

The computational model, Pusan National University Direct-Connect Scramjet Combustor (PNU-DCSC), which is a gaseous hydrogen-fueled direct-connect scramjet combustor, is illustrated in Fig 1. The PNU-DCSC consists of a rocket-type vitiation air heater (VAH), shape transition nozzle [21,22], and scramjet combustor. The cross-sectional of the isolator is a 20 mm x 20 mm. The scramjet combustor has a design point with a Mach number of 2.0 and a static temperature of 1,000 K at the nozzle exit and the isolator entrance. More detailed information on PNU-DCSC and preliminary experiments is described in our previous study [23,24].

To check the grid sensitivity, we set approximately 7.0, 16.0, 34.0, and 62.0 million grids as coarse, medium, fine, and superfine grid levels. The fine and superfine grids achieved a converged solution. We also confirmed that these results agree with the experimental wall pressure profile. The present simulation used the fine grid level, consisting of a fully structured grid with 34.0 million grid points. The computational domain is divided into 1,034 blocks, and each block is handled by intel Xeon Gold 6154 CPUs for MPI parallel calculation.

The present study considered a total of six working fluid conditions. Two incoming air conditions are considered. One is vitiated air, and the other is clean air. In order to investigate the effect of a global equivalence ratio depending on incoming air conditions, injection pressure conditions are set by 1.0, 1.5 and 3.0 bar. More detailed information on working fluid is noted in Table 1.

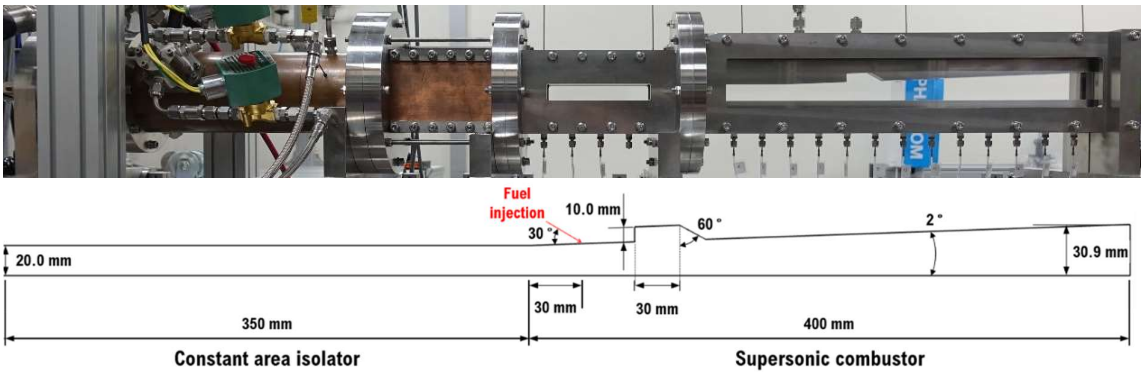

Fig. 1 (top) Experimental test rig of the PNU-DCSC, (bottom) configuration of entire computation domain and its specific size

Table 1. Inflow and fuel injection

	Inflow condition (isolator inlet) Mach#: 2.0 T_{static}: 1007.7 K P_{static}: 2.29 bar	Fuel injection (at port exit) Mach#: 2.15 T_{static}: 151.23 K
	▼ Mole fraction	▼ Injection pressure
Case 1-1	Vitiated air N_2 : O_2 : H_2O = 0.60805 : 0.20353 : 0.18842	1.0 bar (ER≈0.17)
Case 1-2		1.5 bar (ER≈0.25)
Case 1-3		3.0 bar (ER≈0.50)
Case 2-1	Clean air N_2 : O_2 : H_2O = 0.7808 : 0.2192 : 0.0000	1.0 bar (ER≈0.18)
Case 2-2		1.5 bar (ER≈0.26)
Case 2-3		3.0 bar (ER≈0.53)

3. Numerical Results

Field data of entire cases was accumulated up to approximately 10.0 ms (millisecond). It took around 2.0 ms for the stabilized supersonic flow field. Therefore, the fuel was injected after the 2.0 ms. The total sampling time of reactive flow field data is approximately 8.0 ms. The present combustor's flow-through time (FTT) is around 0.2 ms; therefore, reactive flow field data is accumulated during 40 FTT.

Before investigating the vitiation air effect, we sought to confirm the overall combustion characteristics. The instantaneous dimensionless heat release rate distribution is depicted in Fig 2. The distribution of heat release rates can characterize a flame length and the combustion mode, so the heat release rates for all conditions were plotted. The results of the heat release rate indicate that all conditions exhibit a jet-wake combustion mode. This is due to sufficiently high-enthalpy incoming air condition, which derive an auto-ignition.

The time-averaged results for fuel mass fraction and dimensionless vorticity under all conditions were plotted in Fig. 3. Regardless of the changes in the incoming air, the injected fuel shows the same dynamic characteristics of a jet, such as a Counter-Rotating Vortex Pair (CRVP), and exhibits similar hydrodynamic jet behaviors. No significant changes are observed under low equivalence ratio conditions. However, at higher equivalence ratio conditions, a relatively higher fuel mass fraction along the jet core is captured in the vitiated air condition. This suggests that in this region, less fuel consumption has occurred in the vitiated air condition compared to the clean air condition. From a combustion

perspective, this can lead to the expectation that the clean air condition causes a higher rise in combustion pressure in the region between the cavity close-out from the fuel injector.

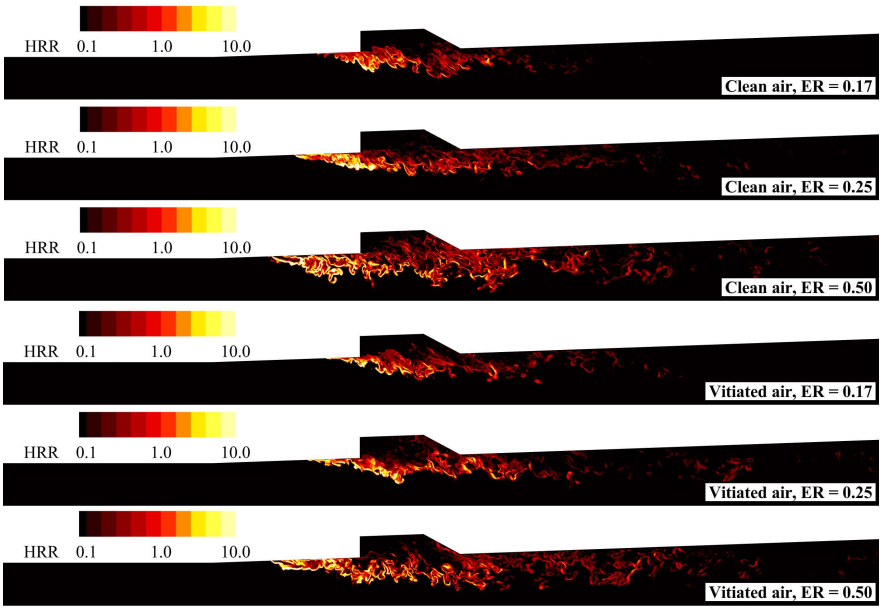

Fig. 2 Instantaneous results of heat release rate distribution; (top) clean air condition, (bottom) vitiated air condition.

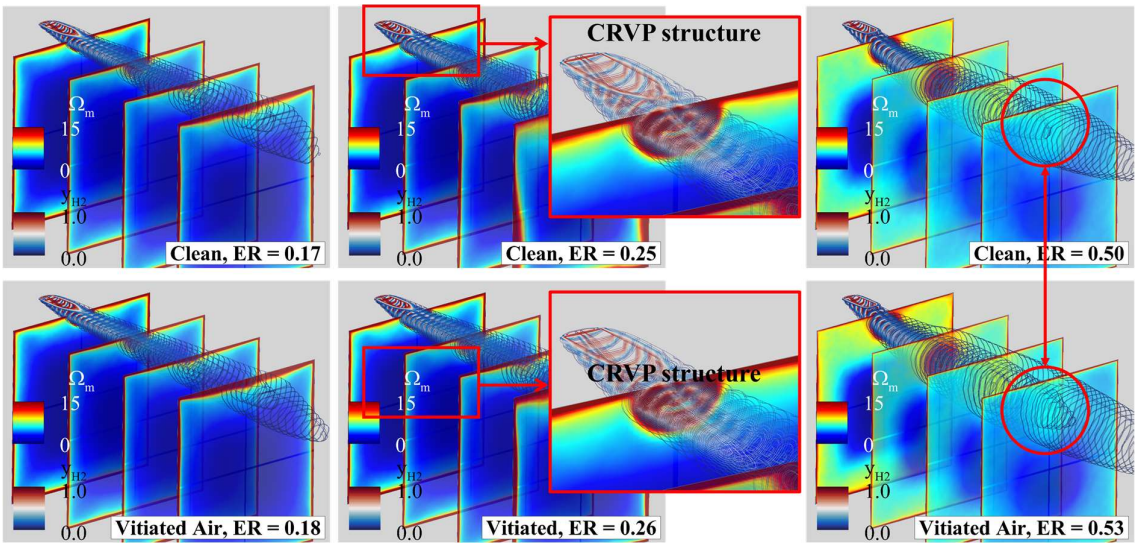

Fig. 3 Time-averaged results of dimensionless heat release rate (contour) and fuel mass fraction (iso-line) distribution; (top) clean air condition, (bottom) vitiated air condition.

Fig. 4 shows an x-t plot of the pressure distribution on the combustor lower wall. There are no captured upstream-traveling shock waves that would induce pressure propagation into the isolator, which is a key factor in low-frequency instability [25,26]. Therefore, the entire case is under a stabilized reacting flow field with the jet-wake combustion mode. Under low equivalence ratio conditions, changes in the composition of the incoming air do not induce significant changes in the pressure field. However, as the equivalence ratio increases, there is an elevation in the level of the pressure field, especially a high-pressure field forms in the upstream area of the combustor, the region between the fuel injector and the cavity close-out.

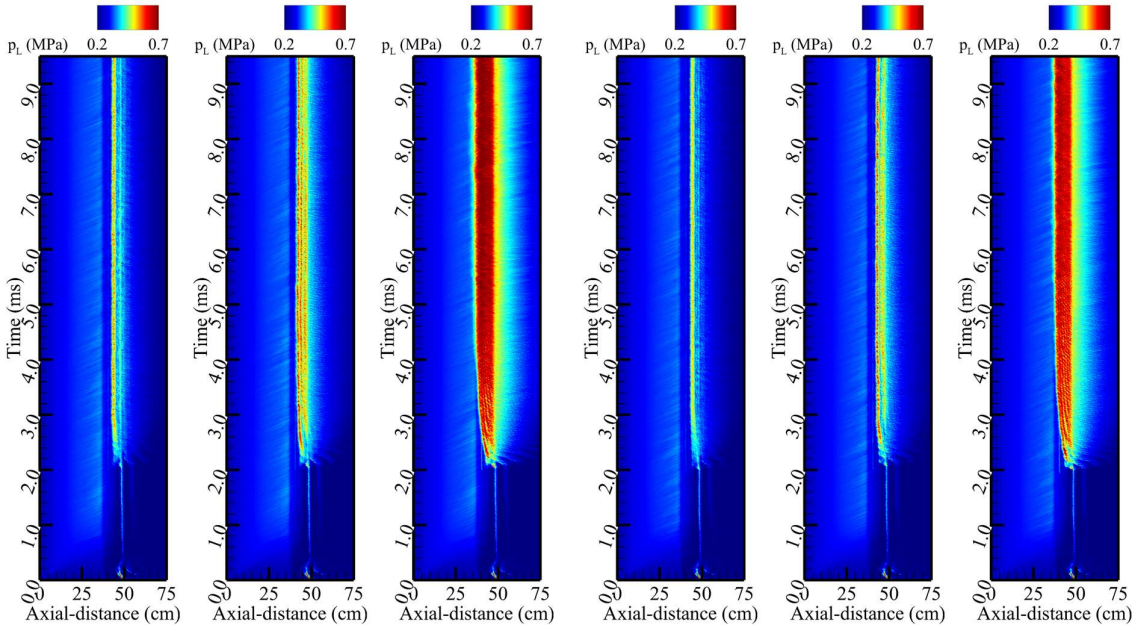

Fig. 4 x-t diagram of the pressure distribution on the lower wall surface. The left three results are under the clean air condition, and the right three results are results of the vitiated air condition. The equivalence ratio increases from left to right of each contour.

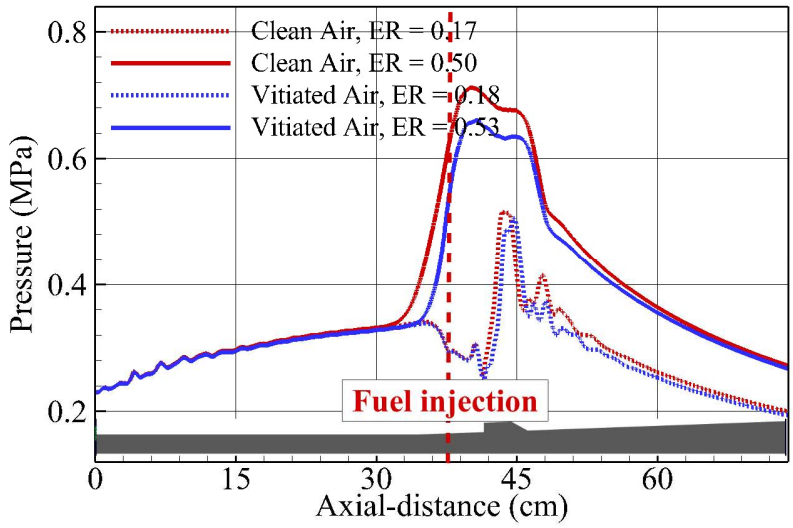

Fig. 5 Pressure field distribution on the lower wall surface of the combustor.

Fig. 4 demonstrates that the intensification of the pressure field occurring under high equivalence ratio conditions and changes in the chemical composition of the incoming air are concentrated in the upstream region of the combustor. In contrast, the effects of the incoming air induce very little change in the pressure field on the combustor downstream. This result can also be observed in Fig. 5, which depicts the pressure field profile on the bottom wall surface.

The lower wall pressure contour indicates that changes in the combustion field due to the incoming air are insignificant under low equivalence ratio conditions. However, under high equivalence ratio conditions, as shown in Fig. 4, there is an increase in the pressure field level, and this increased pressure field predominantly affects the combustor upstream region. Additionally, in the case of the clean air, it can be observed that the region of the axial location where combustion pressure rises sharply moves

further upstream. Although the pressure field does not propagate to the isolator, indicating that it cannot be considered a complete transition to ram mode, it is evident that the formation of pre-combustion shock waves and their expansion upstream are significantly affected by the chemical composition of the incoming air.

The results of the Mach number and temperature fields at an equivalence ratio of about 0.50, extracted from the center of the combustor, are presented in Fig. 6. Under clean air conditions, the flow decelerated down to Mach 1.0 due to a continuous shock train. Subsequently, the flow accelerates to supersonic in the downstream area of the combustor due to its expansion of the combustor. In contrast, the flow decelerates only to about 1.1 under vitiated air conditions, indicating that the flow speed is more than 10% different compared to clean air. As for the temperature field, a consistent difference of about 100 K is shown throughout the downstream of the combustor.

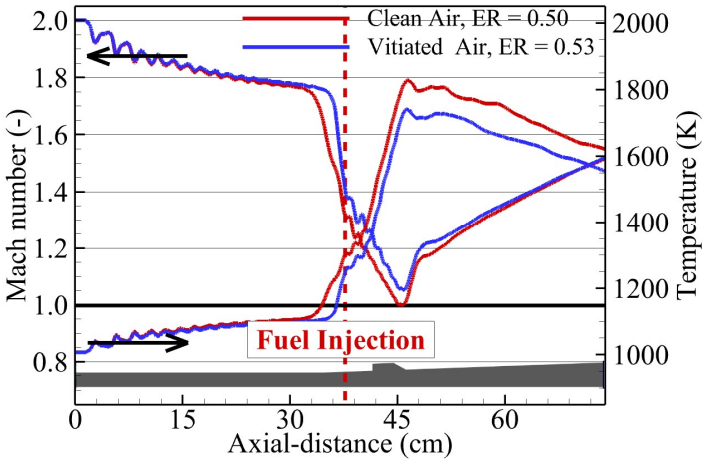

Fig. 6 Mach number and temperature distribution at the core of the combustor along the combustor axial-distance.

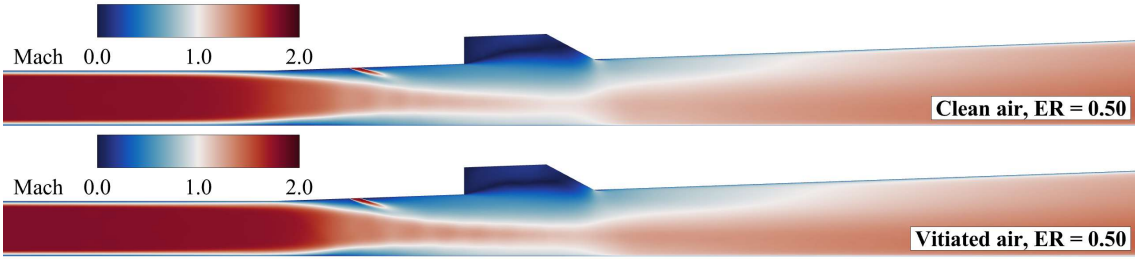

Fig. 7 Time-averaged results of Mach number distribution at the center plane.

The time-averaged Mach number results in Figure 7 effectively illustrate the changes in the location of pre-combustion shock wave formation. For both incoming air conditions, the formation of pre-combustion shock waves accompanied by thermal choking can be observed. However, as the incoming air changes from vitiated air to clean air, the location of pre-combustion shock wave formation significantly shifts towards the isolator. Furthermore, Fig. 8, which illustrates the formation process of pre-combustion shock waves in clean air conditions, reveals that it only takes a few milliseconds to fully develop pre-combustion shock waves.

Owing to the present study's results being based on a total sampling time of 8 ms, it is assessed that there is a very low possibility of further development of these pre-combustion shock waves or a transition to ram mode due to continuous heat release. However, the results of this study indicate that the formation of combustion pressure, caused by the shortened ignition delay time with the clean air,

brings about significant changes in the upstream rather than the downstream area of the combustor. This could potentially lead to increased pressure in the isolator, which, in turn, could result in low-frequency combustion instability in scramjets or even lead to inlet unstart. Therefore, it is deemed necessary to develop theoretical-experimental or numerical correction tools that can adjust ground combustion test results using VAH with combustion products in the intake air, keeping in mind that results under the vitiated air conditions may underpredict actual flight conditions.

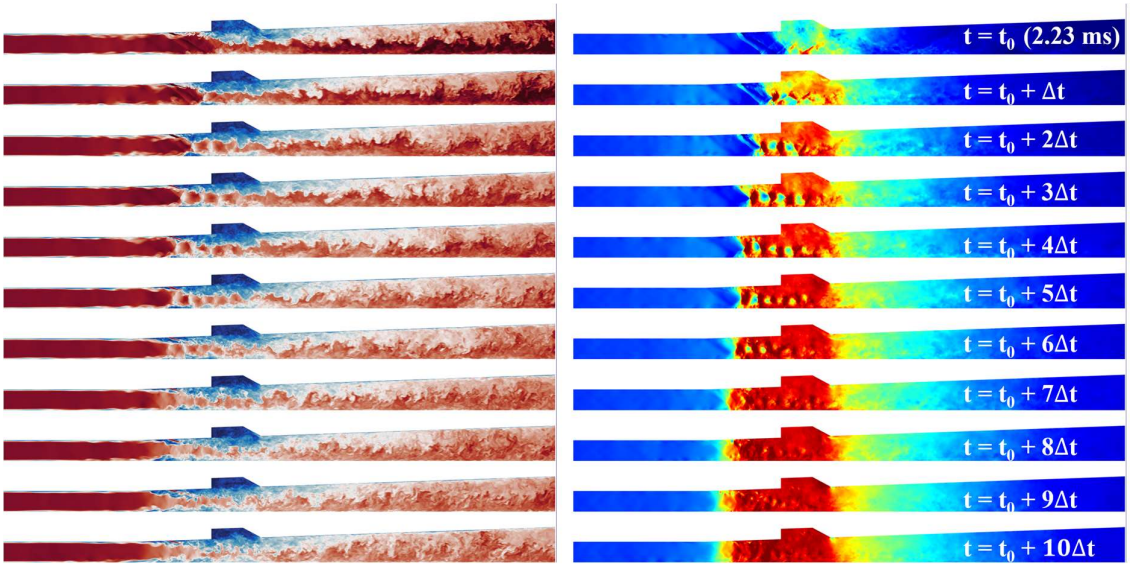

Fig. 8 Evolution process of shock train to pro-combustion shock waves under the clean air condition; (left) Mach number, (right) pressure field distibution. △t is 0.29 ms (milli-second).

Acknowledgement

This work was supported by "A Study on Key Technologies for Hypersonic Future Aircraft" of the Korea Aerospace Research Institute (KARI) (Grant No. FR24L01). This work was also supported by the National Supercomputing Center (NSC) with supercomputing resources including technical support (Grant No. KSC-2022-CRE-0304).

References

1. Noda, J., Tomioka, S., Izumikawa, M., Goyne, C. P., Rockwell Jr, R. D., Masuya, G.: Estimation of Enthalpy Effects in Direct-Connect Dual-Mode Combustor. J. Thermal Sci. Technol. (2011). https://doi.org/10.1299/jtst.6.289
2. Rockewell Jr, R. D., Goyne, C. P., Haw, W., Krauss, R. H, McDaniel J. C., Trefny C. J., : Experimental Study of Test-Medium Vitiation Effects on Dual-Mode Scramjet Performance. J. Propuls. Power (2011). https://doi.org/10.2514/1.B34180
3. Mitani, T., Hiraiwa, T., Sato, S., Tomioka, S., Kanda, T., Tani, K.: Comparison of Scramjet Engine Performance in Mach 6 Vitiated and Storage-Heated Air. J. Propuls. Power (2012). https://doi.org/10.2514/2.5228
4. Feiteng, L., Wenyan, S., Zhiqiang, Z., Weiqiang, L., Jianping, L.: Experimental and Numerical Studies of Vitiated Air Effects on Hydrogen-fueled Supersonic Combustor Performance. Chinese J. Aeronaut (2012). https://doi.org/10.1016/S1000-9361(11)60375-0

5. Haw, W. L., Goyne, C. P., Rockwell, R. D., Krauss, R. H., McDaniel, J. C.: Experimental Study of Vitiation Effects on Scramjet Mode Transition. J. Propuls. Power (2011). https://doi.org/10.2514/1.49090
6. Hash, C. A., Drummond, P. M., Edwards, J. R., Kato, N., Lee, T.: Numerical simulation of stable and unstable ram-mode operation of an axisymmetric ethylene-fueled inlet-isolator-combustor configuration. Combust. Flame (2022). https://doi.org/10.1016/j.combustflame.2022.112157
7. Choi, J.-Y., Jeung, I.-S., Yoon, Y.: Unsteady-state simulation of model ram accelerator in expansion tube, AIAA J. (1999). https://doi.org/10.2514/2.770
8. Choi, J.-Y., Jeung, I.-S., Yoon, Y.: Scaling effect of the combustion induced by shock-wave boundary-layer interaction in premixed gas. Symposium (International) on Combust. (1998). https://doi.org/10.1016/S0082-0784(98)80067-2
9. Choi, J.-Y., Jeung, I.-S., Yoon, Y. B.: Computational Fluid Dynamics Algorithms for Unsteady Shock-Induced Combustion, Part 1: Validation. AIAA J. (2000). https://doi.org/10.2514/2.1112
10. Choi J.-Y., Jeungt I.-S., Yoon Y.B.: Computational fluid dynamics algorithms for unsteady shock-induced combustion, Part 2: comparison. AIAA J. (2000). https://doi.org/10.2514/2.1087
11. Choi, J.-Y., Ma, F., and Yang, V.: Combustion oscillations in a scramjet engine combustor with transverse fuel injection. Proc. Combust. (2005). https://doi.org/10.1016/j.proci.2004.08.250
12. Shin, J.-R., Cho, D.-R., Won, S.-H., Choi, J.-Y.: Hybrid RANS/LES study of base-bleed flows in supersonic mainstream. AIAA 2008-2588. https://doi.org/10.2514/6.2008-2588
13. Shin, J.-R., and Choi, J.-Y.: Dynamic Correction of DES Model Constant for the Advanced Prediction of Supersonic Base Flow," J. KSAS (2010). https://doi.org/10.5139/JKSAS.2010.38.2.099
14. Pavalavanni, P.K., Sohn, C.H., Lee, B.J., Choi, J.-Y.: Revisiting unsteady shock-induced combustion with modern analysis techniques, Proc. Combust. (2019). https://doi.org/10.1016/j.proci.2018.07.094
15. Jeong, S.-M., Choi, J.-Y.: Combined diagnostic analysis of dynamic combustion characteristics in a scramjet engine. Energ. (2020). https://doi.org/10.3390/en13154029
16. Kim, J.–E., Jeong, S.–M., Kim, W.D., Choi, J.–Y., Hwang, Y.: Numerical analysis of internal flow thermal environment in an accelerating high–speed vehicle. Aerosp. Science and Technol. (2024) https://doi.org/10.1016/j.ast.2024.108889
17. Jachimowski, C.J.: An analytical study of the hydrogen-air reaction mechanism with application to scramjet combustion. Report No. L-16372 (1988).
18. Peterson, D.M.: Simulation of a Round Supersonic Combustion using Wall-modeled Large-eddy Simulation and Partially Stirred Reactor Model. Proc. Combust. (2023). https://doi.org/10.1016/j.proci.2022.08.120
19. Gonzalez-Juez, E.D., Kerstein, A.R., Ranjan, R., Menon, S.: Advances and Challenges in Modeling High-speed Turbulent Combustion in Propulsion Systems. Prog. Energy Combust. Sci. (2017). https://doi.org/10.1016/j.pecs.2016.12.003
20. Choi, J.-Y., Unnikrishnan, U., Hwang, W.-S., Jeong, S.-M., Han, S.-H., Kim, K. H., Yang, V.: Effect of Fuel Temperature on Flame Characteristics of Supersonic Turbulent Combustion. Fuel (2022). https://doi.org/10.1016/j.fuel.2022.125310
21. Sung, B.-K., Jeong, S.-M., Choi, J.-Y., Direct-connect supersonic nozzle design considering the effect of combustion, Aerospace Science and Technology, 2023, 133, 108094. https://doi.org/10.1016/j.ast.2022.108094

22. Sung, B.-K., Hwang, W.-S., Choi, J.-Y. Design of a Shape Transition Nozzle for Lab-scale Supersonic Combustion Experimental Equipment J. of the Korean Society for Aeronautical and Space Sciences, 2020, 48(3), pp. 207–215. https://doi.org/10.5139/JKSAS.2020.48.3.207

23. Lee, J.-H., Lee, E.-S., Han, H.-S., Kim, M.-S., Choi, J.-Y.: A study on a vitiated air heater for a direct-connect scramjet combustor and preliminary test on the scramjet combustor ignition. Aerospace (2023). https://doi.org/10.3390/aerospace10050415

24. M.-S. Kim, Koo, I.-H., Lee, K.-H, Lee, E.-S., Han, H.-S., Jeong, S.-M., Kim, H. Choi, J.-Y.: Experimental study on the ignition characteristics of scramjet combustor with tandem cavities using micro-pulse detonation engine. Aerospace (2023). https://doi.org/10.3390/aerospace10080706

25. Jeong, S.-M., Lee, J.-H., Choi, J.-Y.: Numerical investigation of low-frequency instability and frequency shifting in a scramjet combustor. Proc. Combust. (2023). https://doi.org/10.1016/j.proci.2022.07.245

26. Jeong, S.-M., Han, H.-S., Sung, B.-K., Kim, W., Choi, J.-Y.: Reactive Flow Dynamics of Low-Frequency Instability in a Scramjet Combustor. Aerospace (22023). https://doi.org/10.3390/aerospace10110932